Fluorescence lifetime imaging microscopy (flimscopy)

Methodology development and application to studies of endosome fusion in single cells

Takatoku Oida, Yasushi Sako, and Akihiro Kusumi
Department of Pure and Applied Sciences, The University of Tokyo, Meguro-ku, Tokyo 153 Japan

ABSTRACT A new method of fluorescence microscopy for cell imaging has been developed that takes advantage of the spatial variations of fluorescence lifetimes in single cells as a source of image contrast, and thus it is named "fluorescence lifetime imaging microscopy (flimscopy)". Since time-resolved fluorescence measurements are sensitive to molecular dynamics and interactions, flimscopy allows the molecular information to be visualized in single cells. In flimscopy measurements, several (nanosecond) time-resolved fluorescence images of a sample are obtained at various delay times after pulsed laser excitation of the microscope's entire field of view. Lifetimes are calculated pixel-by-pixel from these time-resolved images, and the spatial variations of the lifetimes are then displayed in a pseudocolor format (flimscopy image). The total data acquisition time needed to obtain a flimscopy image *with the diffraction-limited spatial resolution* ($\approx$250 nm) is decreased to just $\approx$30 s for $\approx$300 fluorescent molecules/μm^2. This was achieved by developing a high-frequency (400 kHz) nanosecond-gating (9 ns full width at half height)-signal accumulation system. This technique allows the extent of resonance energy transfer to be visualized in single living cells, and is free from the errors due to variations in path length, light scattering, and the number of fluorophores that necessitate complex corrections in steady-state microfluorimetry and fluorescence ratio imaging microscopy. Flimscopy was applied here to observe the extent of fusion of individual endosomes in single cells. Results revealed the occurrence of extensive fusion between primary endocytic vesicles and/or sorting endosomes, thereby raising the possibility that the biogenesis of sorting endosomes involves multiple fusions of primary endocytic vesicles.

INTRODUCTION

Recent technological developments in time-resolved microscope fluorimetry have enabled the measurement of fluorescence lifetimes in submicrometer regions. Initial applications indicate that microscopic fluorescence lifetime measurements are a powerful, noninvasive method for obtaining information at the molecular or nanometer level (using resonance energy transfer) on biophysical and biochemical processes occurring in single living cells while the subcellular structures of interest are being viewed under a fluorescence microscope with a high-power objective lens (4–7).

Time-resolved fluorescence measurements are essentially more advantageous than steady-state measurements. They can intrinsically provide much more molecular information than do steady-state techniques (8). In the case of microscopic measurements in particular, time-resolved technique is superior because lifetime measurements do not suffer from the inherent drawbacks in the steady-state microfluorimetry associated with complex corrections necessitated by spatial variations in path length, light scattering, and the number of fluorophores. In fact, the excited-state lifetime would be the only physical observable, the absolute value of which could be precisely determined under the fluorescence microscope.

The major problem of carrying out time-resolved microfluorimetry lies in the technical difficulties to obtain a sufficient signal-to-noise (S/N) ratio. Thus, improving instrument sensitivity is a key step for further development of time-resolved fluorescence microscopy. Time-resolved fluorescence measurements in a micrometer region under the microscope have been pioneered by Sacchi (9–12), and Fernandez and his collaborators (4, 5, 13, 14). Alsins et al. (15) and Minami and his coworkers (16) also described instrumentation for time-resolved microfluorimetry. Kusumi et al. (6, 7, 17) further advanced the method via improvements in instrument sensitivity by interfacing the fluorescence microscope to a specially designed synchroscan streak camera. This system reduced the signal acquisition time to 2–60 s for $\approx 10^3$ fluorophores/μm^2, hence making time-resolved microscope fluorimetry a practical technique for biomedical research, e.g., *in situ* endosome fusion has been observed in single cells. Although these developments were made for lifetime measurements in a small region under a microscope, they suggested the possibility of generating microscopic images on the basis of fluorescence lifetime.

We now report the first microscopic imaging of cells that is based on spatial variations in fluorescence lifetime, being termed "fluorescence lifetime imaging microscopy (flimscopy)". Since time-resolved fluorescence measurements are sensitive to molecular dynamics and interactions, flimscopy allows the molecular information to be visualized in single cells. In this paper, we present a detailed description of the instrument, its performance, characteristic features, and limitations as well as its initial application to the studies of cellular membranes, i.e., endosome-endosome fusion in single cells.

In flimscopy measurements, several (nanosecond) time-resolved fluorescence images of a sample with the

Preliminary accounts of this paper have been presented in the 28th Annual Meeting of the Japanese Biophysical Society (1), the 44th Annual Meeting of the Japanese Society for Cell Biology (2), and the 32nd Annual Meeting of the American Society for Cell Biology (3).

Address correspondence to A. Kusumi.

0006-3495/93/03/676/10 $2.00

diffraction-limited spatial resolution are obtained at various delay times after pulsed laser excitation of the microscope's entire field of view. The lifetimes are subsequently calculated pixel-by-pixel, and then their spatial variations are displayed in a pseudocolor or a contour-map format (flimscopy image). The total data acquisition time needed to obtain a flimscopy image with the diffraction-limited spatial resolution of $\approx$250 nm has been decreased to just 30 s for $\approx$300 fluorophores/μm^2. This was achieved by developing an electronic gating system installed in the detection arm which enables rapid accumulation of the time-resolved images at a rate of 400 kHz, consequently improving the S/N ratio of the resultant time-resolved image by a factor of 630 during the first second of signal accumulation.

Similar lifetime images can be generated using the time-resolved microscope fluorimeter (which measures the lifetime in a small region under the microscope) by scanning the laser spot on the sample (6) (Hamamatsu Photonics data sheet No. ETV-188), yet a much longer time is required to form an image. Several papers have been published that described fluorescence lifetime imaging (18, 19), but not fluorescence lifetime imaging *microscopy*. The latter is technically much more demanding. The goal of the present research is (*a*) to achieve flimscopy with the diffraction-limited spatial resolution with high-power objectives, (*b*) to make flimscopy a practical approach for biological problems by reducing the data acquisition time to 3-30 s, and (*c*) to apply flimscopy to observe endosome-endosome fusion in single cells in order to show its usefulness and to contribute to understanding of the initial stages of endocytic processes.

Time-resolved phosphorescence and delayed fluorescence imaging *microscopy* involving slower (millisecond range) luminescence has been reported previously (20). In the present work, the sensitivity and time resolution have been improved considerably to enable flimscopy measurements.

The flimscopy technique allows the spatial variations in the extent of resonance energy transfer (which reduces the lifetime of the energy donor) to be visualized in single living cells. Since flimscopy images are based on fluorescence lifetimes, they are free from the errors due to the spatial variations in path length, light scattering, etc., thus making flimscopy a more preferable technique than conventional fluorescence ratio imaging microscopy.

Flimscopy has made possible a new method for observing endosome fusion in single cells. The extent of fusion, and fused and unfused endosomes have been clearly visualized. The application of flimscopy has indicated the occurrence of extensive fusion between primary endocytic vesicles and/or between sorting endosomes, which raises the possibility that the biogenesis of sorting endosomes involves multiple fusions of primary endocytic vesicles.

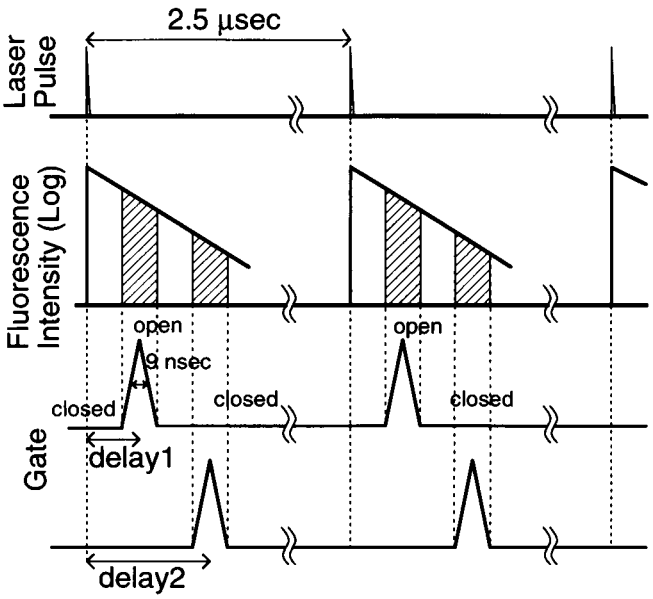

FIGURE 1 A timing diagram showing pulsed laser excitation, resultant fluorescence emission, and operation of the nanosecond gate. A train of laser pulses illuminates the microscope's entire field of view, a portion of the fluorescence decay is selected by the gate, and the fluorescence signal that passes the selected time window of the gate is accumulated by a slow-scan, cooled CCD camera. The typical accumulation time for each time-resolved image ranges from 0.5 to 10 s. This procedure is repeated at various delays between the pulsed excitation and the opening of the gate (delay 1, delay 2, . . .).

MATERIALS AND METHODS

Flimscopy measurements

Fig. 1 shows a timing diagram of pulsed laser excitation, fluorescence emission, and operation of the nanosecond gate. A train of laser pulses (λ = 488 nm, full width at half height (FWHH) $\approx$ 400 psec, repetition rate = 400 kHz, average power $\approx$ 35 mW) illuminates the microscope's entire field of view, a portion of the fluorescence decay is selected with the gate (FWHH $\approx$ 9 ns), and the fluorescence signal that passes the selected time window of the gate is intensified with a microchannel plate (MCP) and then accumulated by a slow-scan, cooled, charge-coupled device (CCD) camera. Typical accumulation time for obtaining each time-resolved image is 0.5–10 s ($0.2–4 \times 10^6$ additions of the signal). This procedure is repeated at various delay times between the pulsed excitation and the opening of the gate (delays 1, 2, . . . , in Fig. 1). Fluorescence lifetimes are calculated pixel-by-pixel using several (4–7) time-resolved images. In general, the more points are taken, the estimate of the lifetime is better, as long as the bleaching of the sample is not serious and the data acquisition time is within the practical range. To alleviate the effect of sample photobleaching on the estimate of lifetimes, the delay times were cycled and the time-resolved image at each delay time was measured twice, i.e., measuring from the shortest (first) delay time and increasing to the longest (last) delay time, and then measuring from the longest delay time and decreasing to the shortest delay time.

The configuration of the instrument we have developed for flimscopy is shown in Fig. 2. The instrument consists of five major components: (*a*) a pulsed light source, (*b*) a fluorescence microscope equipped with epi-illumination capability and filter sets for selection of limited spectral regions, (*c*) a nanosecond gated image intensifier and the gate driver, (*d*) a slow-scan cooled CCD camera for on-chip accu-

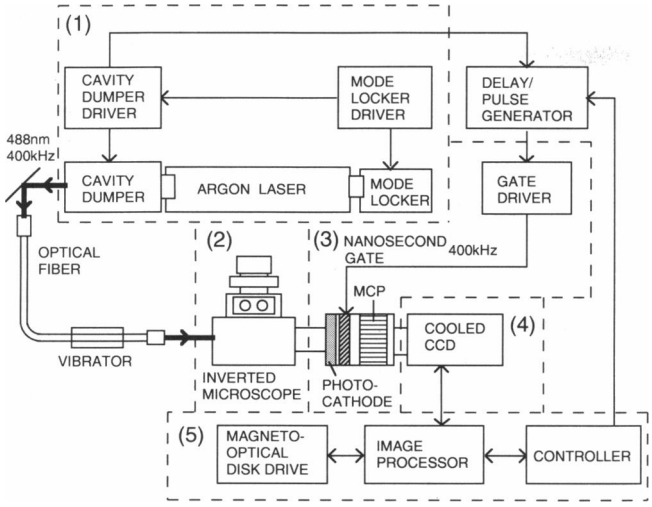

FIGURE 2 (A) A schematic diagram of the time-resolved fluorescence microscope (flimscopy instrument). The pulsed light source (*1*) is a cavity-dumped, mode-locked argon ion laser, which illuminates the entire field of view of the microscope (*2*). Time-resolved fluorescence microscopic images are obtained with a nanosecond electronic gate (*3*) which operates synchronously with the laser excitation at specifically set time delays. Time-resolved images are then intensified with an MCP and accumulated on the cooled CCD chip of a slow-scan, cooled CCD camera (*4*). The gate driver was specially designed to increase the repetition rate of the signal acquisition sequence. The experiment is completely controlled by a personal computer used in conjunction with an image processor (*5*). The acquired images are transferred to a computer for calculation of fluorescence lifetimes and image reconstruction.

mulation of the time-resolved image, and (*e*) a computer for controlling the experiments and for analyzing the fluorescence decay data to reconstruct flimscopy images.

Details of each component are as follows: (*a*) The pulsed light source is a cavity-dumped mode-locked argon ion laser (models 2025, 342A-01, 453, 341-02, and 344-01S, Spectra Physics, Mountain View, CA). Light pulses are guided onto the optical axis of the microscope using a multimode optical fiber and a beam steering unit. (*b*) A Zeiss Axiovert fluorescence microscope (Oberkochen, Germany) is employed. The laser beam is adjusted to illuminate the microscope's entire field of view using a focusing lens placed just before the entrance of the microscope. A Zeiss 100× Plan-Neofluar objective lens (N. A. = 1.30) was used throughout this study. Interference and long-pass filters were purchased from Zeiss, Nihon-shinku (Tokyo, Japan), and Fuji Film (Tokyo, Japan). (*c*) Time-resolved fluorescence microscopic images are obtained using a nanosecond gated image intensifier (Hamamatsu Photonics V3063U; Hamamatsu, Japan) which is installed in the microscope's detection arm. The gate is synchronized with the laser pulse excitation at a defined delay time using a digital delay/pulse generator (Stanford Research, DG535; Sunnyvale, CA), and is operated by varying the voltage (≈200 V) applied to the accelerator grid on the back of the photocathode. The gate driver was specially developed to enable gate operation at a fast repetition rate, which is now 500 kHz at maximum. The high repetition rate and a good gain profile of the gate are not easily compatible: at 2 Hz the gate profile is square-shaped with an FWHH of ≈2.5 ns, but at 400 kHz triangular-shaped with an FWHH of ≈9 ns (see below and Fig. 3). The laser pulse frequency is thus decreased from 4 MHz to 400 kHz at the cavity dumper to match the gate's repetition rate. Time-resolved images are obtained by the combination of the pulse laser and the nanosecond-gated image intensifier.

The system response function was obtained by measuring the reflection from a mirror placed on the microscope stage. A small fraction of the reflected light passed the dichroic mirror, which has sufficient intensity for the present detection system. The barrier filter after the dichroic mirror was removed for this measurement. The delay times between the laser excitation and the opening of the gate were varied. A typical response function is shown in Fig. 3. The profile is stable as long as the laser emission is well adjusted. The major determinants for the system response function (FWHH = 9 ns) are the gain profile of the gate and the laser pulse shape (FWHH ≈ 400 ps), and thereby the limiting factor for the time-resolution of the present instrument is the FWHH of the gate gain profile.

(*d*) The gated and intensified fluorescence images are accumulated by a Hamamatsu cooled CCD camera equipped with a Thomson CCD chip (C3640; cooled to −40°C). When using the Zeiss 100× Plan-Neofluar objective lens, each pixel corresponds to a sample area of 93 × 93 nm^2 with an effective resolution of 1.5 pixels (114 × 114 nm^2). The major determinant for the instrument's spatial resolution is therefore light diffraction.

(*e*) A personal computer (EPSON 286VE) interfaced with a Hamamatsu image processor C4120K-S are used to control the entire experiment, to analyze the time-dependent fluorescence decays, and to reconstruct the flimscopy image. The effective fluorescence lifetime is calculated pixel-by-pixel by assuming a single exponential decay using time-resolved images taken at 4–7 different delay times. This assumption is justified when one of the decay components represents most of the fluorescence intensity, which is often true with organic fluorescent dyes. It should be noted that the effective lifetimes are often sufficient to observe relative changes. Also, curve fitting with two exponentials is not possible since only 4–7 time points are taken. The lifetimes were determined by an iterative least squares analysis with iterative convolution routines using the measured gate profiles (7).

Materials

Utilized materials were obtained from the following sources: *N*-(7-nitrobenz-2-oxa-1,3-diazol-4-yl)dipalmitoyl-L-α-phosphatidylethanolamine (NBD-PE), *N*-(lissaminerhodamine B sulfonyl)dipalmitoyl-L-α-phosphatidylethanolamine (LRB-PE), and sulforhodamine B (SRh) from Molecular Probes (Eugene, OR); calcein from Dojin (Kumamoto, Japan); egg yolk phosphatidylcholine and dimyristoyl-L-α-phosphatidic acid from Sigma (St. Louis, MO); cholesterol (crystallized) from Boehringer (Indianapolis, IN); the minimum essential me-

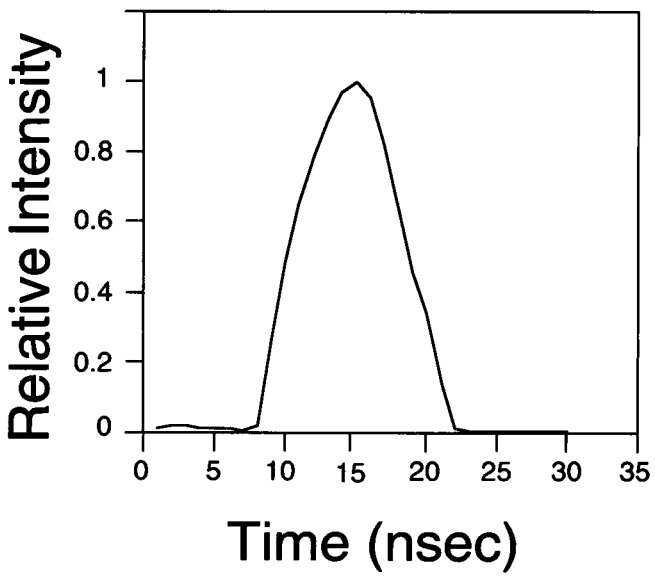

FIGURE 3 The system response function of the flimscopy instrument.

dium (MEM, Earle's salt) from Nissui (Tokyo, Japan); and fetal bovine serum from GIBCO (Grand Island, NY).

Preparation of liposomes

Mixtures of lipids containing only NBD-PE (energy donor) or both NBD-PE and LRB-PE (energy acceptor) (total 5 μmols, NBD-PE:LRB-PE:egg-yolk phosphatidylcholine:cholesterol:phosphatidic acid = 0.1:(0 or 1):70:30:4 by mols) were dissolved in chloroform, dried under a stream of nitrogen gas, and further dried for at least 24 h under a reduced pressure (≈0.1 mmHg). To the thin film of lipids formed at the bottom of the test tube, 1 ml of buffer (2 mM piperidine-*N,N'*-bis(2-ethanesulfonic acid)-NaOH (PIPES), pH 7.1) containing 1 mM ethylenediaminetetraacetic acid and 20 mM glucose was gently added at room temperature. Following incubation for 2 h at room temperature, liposomes released from the glass wall were gently recovered with a Pasteur pipet. The two types of liposomes (with and without 1 mol% of the energy acceptor) were then mixed at a ratio of 1:1 just prior to the flimscopy measurements. Coverslips coated with poly-L-lysine (MW = 15–30 kD) were prepared by incubating the coverslips in 1 mg/ml of poly-L-lysine for 30 min, followed by washing in distilled water. The liposome mixture (5 μl) was placed on the prepared coverslip, mixed with glucose oxidase and catalase (0.1 mg/ml final concentration), and then using the same buffer sealed on a slide glass. These enzymes and the glucose were used to remove molecular oxygen in the sample, and thus prevented photobleaching of the fluorescence (21).

Assay of intracellular endosome-endosome fusion

A normal rat kidney fibroblastic cell line (NRK cells) was routinely maintained in MEM containing 10% fetal bovine serum. This cell line was chosen for this study because these cells were not appreciably affected by low-temperature incubation needed for this experimental procedure. For endocytosis of water-soluble fluorescent probe molecules, NRK cells cultured on coverslips were first incubated in MEM (without phenol red and $NaHCO_3$) containing 5 mM calcein (energy donor) and 5% fetal bovine serum buffered with 2 mM PIPES (pH 7.3) at 18°C for 20 min. After extensive washing of the cells at 4°C using MEM without calcein, the cells were incubated at 18°C in MEM containing 15 mM SRh (energy acceptor) for 0, 5, 10, and 20 min, and were then fixed for 5 min with 2% paraformaldehyde and 0.5% glutaraldehyde in phosphate-buffered saline. Internalization of calcein and SRh was carried out at 18°C so that the observed endosomes would only be primary endocytic vesicles and sorting endosomes, and that fusion with lysosomes would be blocked (22). For the flimscopy measurements, the labeled cells were washed again with MEM and the coverslip was placed upside down on a slide glass with spacers and then sealed in MEM with paraffin.

RESULTS AND DISCUSSION

Flimscopy images of liposomes

Fig. 4 shows the time-resolved images (*a–c*) and a flimscopy image (*d*) of two liposomes.[1] It also serves to show the procedure of the flimscopy measurement. The sample is a mixture of two kinds of liposomes: one type (lower liposome) contains 0.1 mol% of NBD-PE; the other type (upper liposome) contains both 0.1 mol% NBD-PE (energy donor) and 1 mol% LRB-PE (energy acceptor), in which the fluorescence lifetime of NBD-PE would be reduced due to resonance energy transfer to LRB-PE. Figs. 4 a, b, and c, display the time-resolved images of NBD-PE taken at delay times of 4, 8, and 12 ns after laser pulse excitation (no LRB-PE fluorescence was observed with the filter set used). The relative fluorescence intensities of the two liposomes changed dramatically. At the 4 ns delay time, the fluorescence intensity of NBD-PE in the upper liposome is higher than that of the lower liposome (Fig. 4 *a*), becoming nearly similar at the 8 ns delay time (Fig. 4 *b*), and then ending up significantly lower at the 12 ns delay time (Fig. 4 *c*), i.e., the fluorescence lifetime of NBD-PE in the upper liposome is shortened by the presence of the energy acceptor. The effective fluorescence lifetime was calculated at each pixel using time-resolved images taken at 6 different delay times, and a flimscopy image was reconstructed (Fig. 4 *d*). The distinction between the liposomes with and without the energy acceptor is clear. The average fluorescence lifetimes are 7.2 and 4.4 ns for the lower and the upper liposomes, respectively (see the next subsection).

Accuracy of the effective fluorescence lifetime

The fluorescence lifetimes of NBD-PE were measured in a region of ≈13 μm^2 within individual liposomes (containing only NBD-PE) using a time-resolved microscope fluorimeter we previously developed (Kusumi et al., 1990, 1991). Fig. 5 *a* shows a typical lifetime decay, a double-exponential curve with lifetimes of 2.4 and 7.5 ns, with integrated relative intensities of 9 and 91%, respectively.

For comparison purposes, using the time-resolved images from the flimscopy measurements, an average of the fluorescence lifetime decays of NBD-PE in a region of ≈22 μm^2 (51 × 51 pixels) within a liposome was obtained (Fig. 5 *b*). The effective lifetime is 7.2 ns, hence closely agreeing with the decay time of the slower major decay component of NBD-PE.

This agreement may be due to the following: (*a*) the decay signal with the 2.4 ns lifetime is already small at 4 ns, which is the first delay time used in the flimscopy measurements, and (*b*) the major decay component represents more than 90% of the integrated fluorescence intensity. Consequently, for flimscopy it would be convenient to select the energy donors that have a slow decay component representing most of the fluorescence intensity. Further enhancement of the sensitivity of the instrument, along with the availability of faster workstations at lower costs, would make possible multi-component analysis of the fluorescence decay curves and would increase the accuracy in the estimate of fluorescence lifetimes.

The shortest lifetime that can be used for flimscopy with the present instrumentation is somewhat difficult to determine. Flimscopy images of endosomes having an average effective lifetime of ≈1.5 ns were routinely ob-

[1] We refer to the images directly obtained from the instrument (such as those shown in Figs. 4 *a–c*) as "time-resolved images", whereas the reconstructed images from the calculated lifetimes using the time-resolved images are called flimscopy images (Fig. 4 *d*).

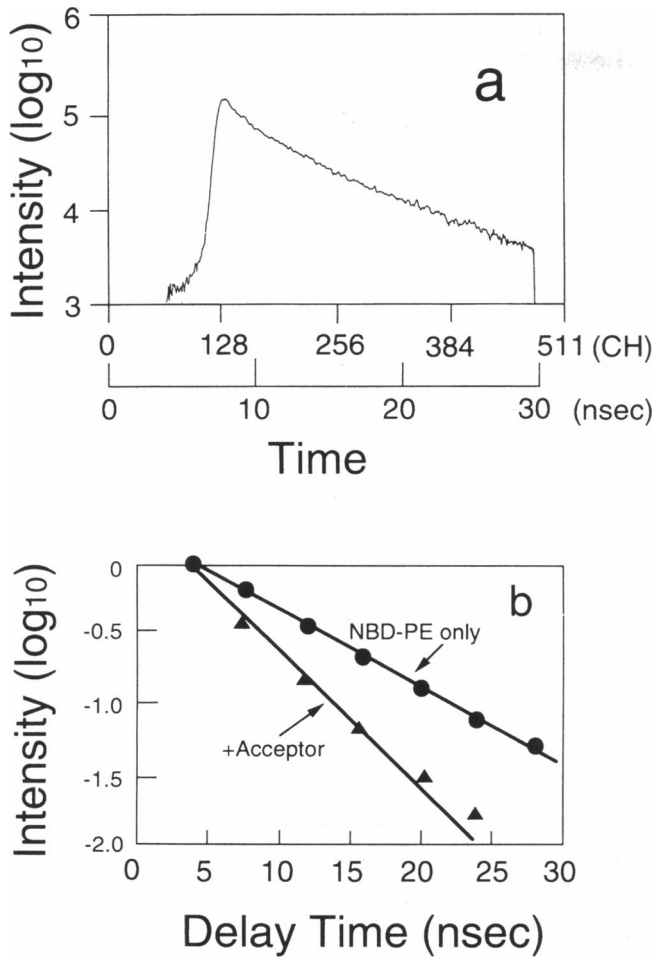

FIGURE 5 (*a*) A typical fluorescence lifetime decay curve of NBD-PE measured in a region of $\approx 13\ \mu m^2$ within a liposome membrane, obtained by a time-resolved microscope fluorimeter we previously developed (Kusumi et al., 1990, 1991). The decay is a double exponential curve with lifetimes of 2.4 and 7.5 ns having integrated relative intensities of 9 and 91%, respectively. (*b*) An average fluorescence lifetime decay of NBD-PE obtained in a region of $\approx 22\ \mu m^2$ (51 × 51 pixels) within a liposome membrane, measured from 7 time-resolved images in flimscopy measurement. The effective lifetime assuming a single exponential is 7.2 ns. Also shown is a corresponding measurement for a liposome containing LRB-PE in addition to NBD-PE, with the effective fluorescence lifetime of 4.4 ns.

served for those containing fluorophores in the order of 10^3–10^4 molecules. Lifetimes comparable to 10% FWHH of the system response function are generally measured in time-resolved fluorimetry (23), and this may be feasible with flimscopy (τ = 0.9 ns) using the existing instrumentation if the signal level is sufficiently high.

Instrument sensitivity

A low S/N ratio is an inherent problem of time-resolved fluorescence microscopy. In the present study, we have largely solved this problem by developing a novel gate operation scheme. Since the S/N ratio can be improved by signal accumulation, and since we are dealing with labile and ever-changing biological samples, we concentrated our effort on performing the signal accumulation (repetition rate) as rapidly as possible.

The devised scheme for improving sensitivity is described as follows (see Fig. 1): (*a*) A gate driver was developed that operates at 400 kHz, thereby improving the S/N ratio of the time-resolved image by a factor of 630 during the first second of image acquisition (e.g., 800,000 additions were carried out during the 2 s acquisition time to obtain each time-resolved image shown in Figs. 4 a–c). (*b*) A satisfactory trade-off between time resolution and instrument sensitivity at the present level of technological development was realized by employing a 9 ns FWHH gate width. (*c*) Rapid yet low-noise signal accumulation was carried out on the cooled CCD chip of a slow-scan CCD camera.

Flimscopy images of reasonable quality were obtained (data not shown) for liposomes containing 0.003 mol% NBD-PE (1/30 the concentration of that used for images in Fig. 4) using an 8 s signal acquisition time for each time-resolved image. Since morphological observations and fluorescence intensity measurements suggested that most liposomes are uni- or bi-lamellar, the instrument sensitivity is estimated to be better than 200–400 NBD molecules/μm^2 (assuming that a lipid molecule in a membrane in the liquid-crystalline phase occupies 0.65 nm^2). Work is now in progress for improving the sensitivity per unit experiment time by increasing the repetition rate to 4 MHz, one which matches the laser's maximum repetition rate after cavity dumping.

Application to studies of intracellular endosome fusion

Flimscopy was applied for quantitative assay of endosome-endosome fusion in NRK cells in culture. To measure the degree of endosome fusion, intermixing of their internal contents was monitored by detecting resultant resonance energy transfer which occurs when endosomes containing the energy donor and those containing the energy acceptor fuse. This transfer is detected as decreases in the fluorescence lifetime of the energy donor. This method has been previously developed by us to observe endosome fusion in single cells using time-resolved microscope fluorimeter (6, 7). The data showed general agreement with the results by Salzman and Maxfield (24), who observed endosome fusion by monitoring quenching of fluorescence by steady-state imaging that is induced by intermixing of fluorescein and anti-fluorescein antibodies separately loaded in sequentially formed endosomes. The validity of the time-resolved resonance energy transfer method to detect vesicle fusion by monitoring intermixing of the internal contents of vesicles was also shown by observing liposome fusion induced by pH-sensitive fusogen, succinylated melittin (7).

According to the employed procedure, endosomes

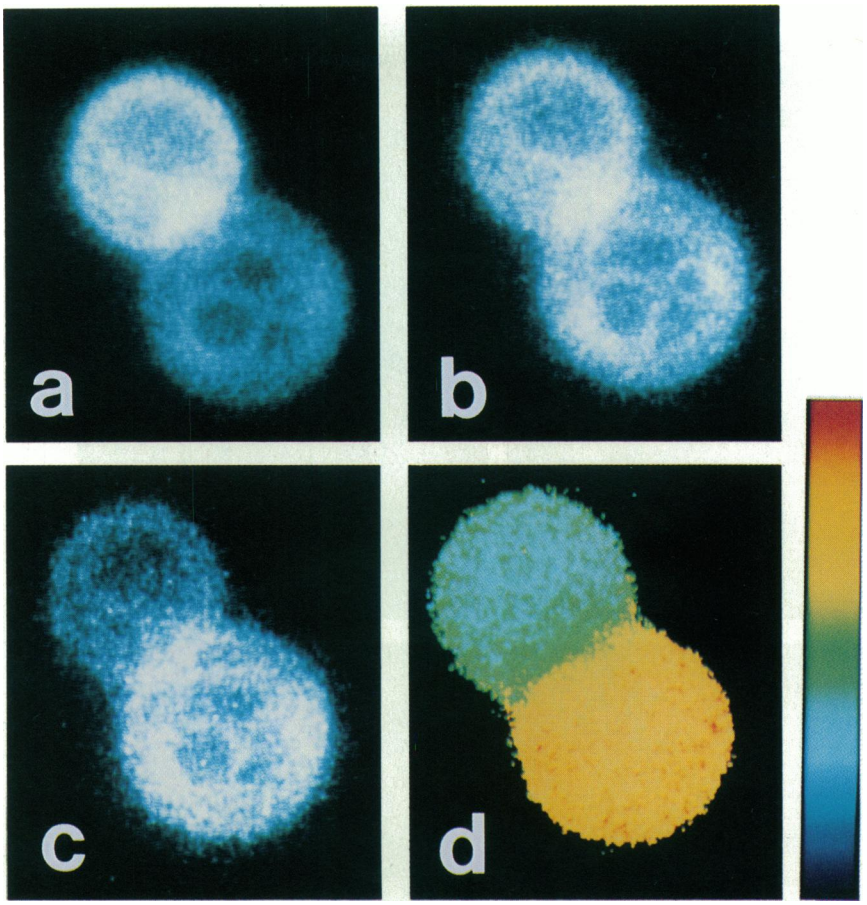

FIGURE 4 Time-resolved fluorescence images of liposomes containing NBD-PE (energy donor) in the presence (upper liposome) and absence (lower liposome) of the energy acceptor, LRB-PE. Time-resolved fluorescence images of NBD-PE were taken at 4 (*a*), 8 (*b*), and 12 (*c*) ns after the excitation laser pulse. The acquisition time for each image was 2 s (800,000 additions). Note only the *relative* fluorescence intensities of the two liposomes at each delay time. The intensities of different figures cannot be compared because the output gain of the computer is increased as the delay time is increased (as the absolute fluorescence intensities decrease). These figures indicate that fluorescence lifetimes of NBD-PE in the upper liposome are shorter than those in the lower one. (*d*) Flimscopy image of the same sample. The color scale indicates from 0 (dark blue) to 11 nsec (red) in the linear scale. Each figure is 15 μm wide.

containing calcein, an energy donor, and those containing SRh, an energy acceptor, in their aqueous phases were sequentially formed. Thus, this method allowed us to examine intracellular fusion of endosomes formed at different times (with time intervals).

In the following experiments, only calcein fluorescence was measured (540 ± 15 nm). Primary endocytic vesicles and sorting endosomes were selectively observed since incubation with the dyes was carried out at 18°C (7, 22). Elongated tubulovesicular bodies (3–10 μm in length) were occasionally observed. However, the tubulovesicular network previously reported in hepatic cells (25) was not observed even in living cells under these experimental conditions.

When an endosome containing calcein fuses with an endosome containing SRh, mixing of the endosomes' internal aqueous contents takes place with the fluorescence lifetime of calcein subsequently decreasing due to energy transfer to SRh. Fig. 6 *a–c,* respectively shows superimposed images of differential-interference contrast and steady-state calcein fluorescence images of NRK cells after incubation with SRh for 0, 10, and 20 min, whereas flimscopy images of the same cells are respectively displayed in Fig. 6, *d–f,* clearly showing the extent of fusion for individual endosomes as well as the distribution of endosomes in single cells.

At early stages after the addition of the energy acceptor, extensive fusion of the endosomes occurs throughout the cell (compare Fig. 6, *d* and *e*). We speculate that this type of early fusion is that occurring between primary endocytic vesicles (differentiation between primary endocytic vesicles and sorting endosomes is not possible in the present experimental scheme). Larger endosomes tend to form near the nucleus within 10 min after internalization of the dye molecules (26) and afterwards fuse more slowly (Fig. 6, *e* and *f*). The number of endosomes per cell decreases, and the number of endosomes with shorter lifetimes increases as the duration of incubation with SRh increases from 10 to 20 min (compare Fig. 6, *e* and *f*). No changes in the fluorescence

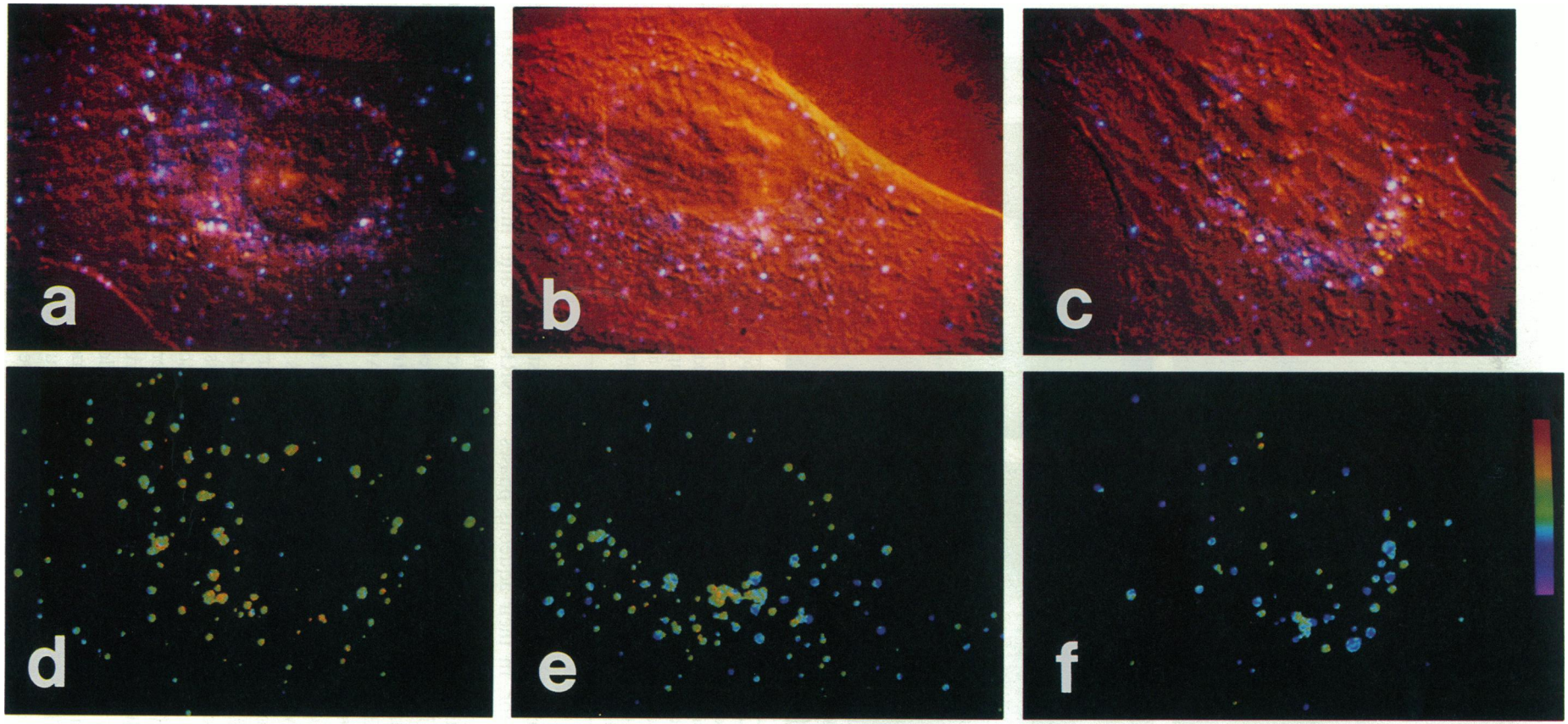

FIGURE 6 (*a–c*) Superimposed microscopic images of differential interference contrast and steady-state fluorescence of NRK cells in culture. The cells were incubated with calcein and then with SRh for 0 (*a*), 10 (*b*), and 20 (*c*) min. (*d–f*) Flimscopy images of the same cells shown in *a–c*, respectively. The color scale indicates from 1 ns (purple, extensive fusion) to 4.5 ns (red, no fusion) on a linear scale. Each figure, except *f*, is 50 μm wide. The scale for *f* is the same as others.

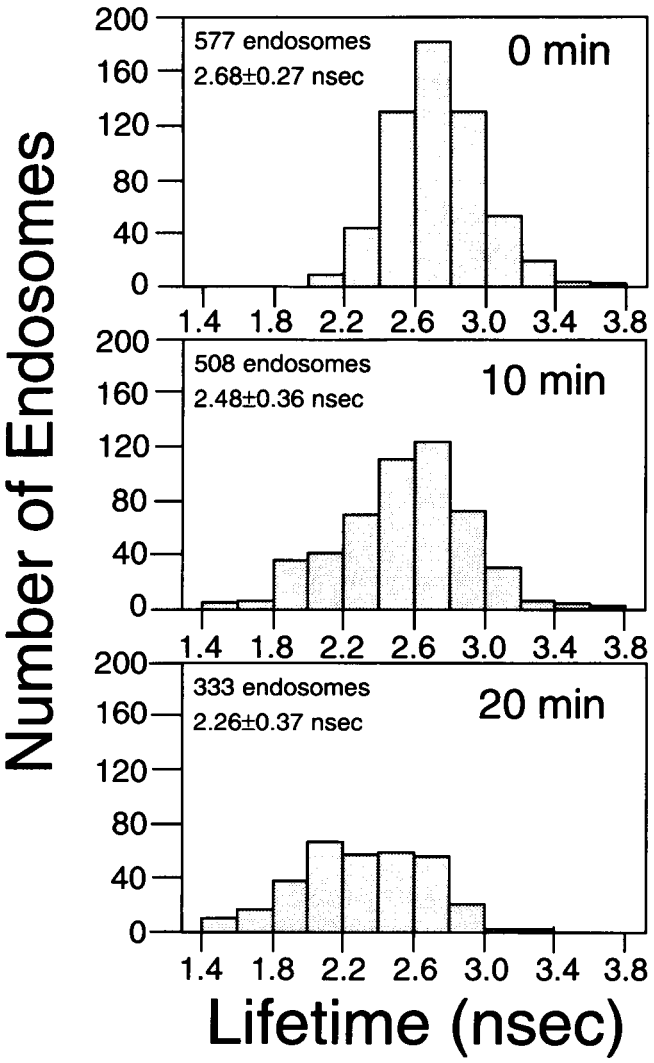

FIGURE 7 A histogram showing the number of endosomes vs. the fluorescence lifetime of calcein in the endosome at various incubation times with SRh. All endosomes observed in seven arbitrarily-selected, typical cells were counted. Note the number of endosomes with shorter lifetimes increases as the incubation duration increases.

lifetimes were observed when the second incubation was carried out in the absence of SRh or in the presence of calcein in place of SRh. When the cells were incubated with SRh without calcein, no fluorescence signal was detected at the present setting of the instrument (using the calcein channel).

Fig. 7 shows histograms of the number of endosomes versus the average fluorescence lifetime of calcein in the endosome for the three incubation times with SRh. All endosomes observable in seven arbitrarily-selected typical cells were counted, i.e., 300–600 endosomes were examined at each time point. This type of measurement is made possible by the development of flimscopy. These histograms quantitatively show decreases in the total number of endosomes and increases in the number of endosomes with short lifetimes (1.4–2.2 ns) with increasing incubation times.

The changes occurring between 10 and 20 min are of particular interest (Fig. 6 *e* and *f*, and Fig. 7, *middle* and *bottom*) since they indicate further fusion among already fused endosomes, i.e., during 20 min, most of the endosomes undergo multiple fusions in which fused primary endocytic vesicles fuse again each other or with the sorting endosomes. It is also possible that sorting endosomes may fuse with each other. Even if the endosomes seen in Fig. 6 *d* are the primary endocytic vesicles, fusion observed at the later stages (10–20 min after addition of SRh) may involve fusion among sorting endosomes. If the endosomes observed in Fig. 6 *d* are already sorting endosomes, these later events indicate fusion among them. The present results support a model in which formation of sorting endosomes involves multiple fusions of many primary endocytic vesicles (7, 27–29).

Comparison with other fluorescence microscopic imaging methods

Dynamic fluorescence measurements by the pulse or the phase method are in general much more informative for observation of dynamic molecular processes, such as resonance energy transfer, molecular rotational diffusion, solvent relaxation, and quenching by molecular collisions, than the steady-state measurements. In particular, we believe that the dynamic measurements are a more sound approach for obtaining molecular information under the microscope by the reasons mentioned in the introduction section.

Experiments for observing endosome fusion can be carried out using steady-state fluorescence microscopic imaging methods. In steady-state imaging, all fluorescence intensity signal is used for imaging, and in principle suited for imaging of distribution of the fluorophores and morphological observation, such as distribution of endosomes in single cells (Fig. 6, *a–c*). In these figures, the fluorescence intensity of calcein in each endosome tends to decrease with time after incubation with SRh, indicating occurrence of resonance energy transfer. However, the intensity by itself also reflects the variation in calcein concentration in individual endosomes, possibly affected by variations in the uptake efficiency of each endosome or leakage of calcein from the endosomes. In addition, the fluorescence intensity is dependent on the size of the endosome. These problems can be alleviated by performing ratio imaging of calcein and SRh. However, by our hands, due to the slight shift and distortion of the images when the dichroic mirrors and the filters are changed for the measurements of calcein and SRh fluorescence, it was difficult to completely match the two images, at the edges of the endosomes in particular due to the sharp rises of the fluorescence intensity. Thus, the absence of such optical components that changes the images in the detection arm is a practical advantage of the present method. (With specimens with more gradual spatial variations of the fluorescence intensity, reason-

able ratio images could be obtained as widely performed.)

The flimscopy would have clearer advantages over the steady-state method for observations of anisotropic depolarization of fluorophores with non-zero limiting anisotropy (r_∞). The resonance energy transfer imaging of samples with heterogeneous distribution of the donor and acceptor, which would have two transfer rates in one pixel, could be performed much better by flimscopy, when its sensitivity is sufficiently improved to allow two-component analysis of the lifetime decays. The present research would form the basis for such development.

Flimscopy images can be obtained using the previously-developed time-resolved microscope fluorimeter (which measures the lifetime in a submicrometer region under the microscope) by scanning the laser spot on the sample (6) (Hamamatsu Photonics data sheet No. ETV-188), yet a much longer time is required to form an image and this method cannot be a practical tool for ever-changing and labile biological samples. However, these studies gave the platform for the present research by providing detailed basic data on the fluorescence lifetime decays obtained from submicrometer regions in cells, individual endosomes, and liposomes that contain fluorescent probes in the lipid bilayer part and in the internal aqueous phase.

Marriott et al. (20) reported time-resolved phosphorescence and delayed fluorescence imaging microscopy involving slower luminescence in the millisecond range. The basic concepts and thrusts for their study is the same as those in this study. Wang et al. (19) also reported fluorescence lifetime imaging, but not microscopy, on non-biological control samples. Their basic instrumental design is similar except the microscope part, but the pulse repetition rate is only 25 Hz, which would not give sufficient sensitivity for microscopy work at the diffraction-limited spatial resolution during a time period meaningful for biological specimens (the nominal spatial resolution of their system is ≈ 5 μm). In the present work, the sensitivity and spatio-temporal resolution have been improved considerably to enable flimscopy measurements.

A possibility of performing lifetime-selective fluorescence imaging using a phase method has been shown by simultaneously imaging two cuvettes containing rhodamine 6G (4 ns lifetime) and rhodamine B (1.5 ns lifetime) (18). The phase modulation method may eventually provide flimscopy images with higher S/N ratio for a given data collection time than the pulse method when it is actually applied for fluorescence microscopy. Meanwhile, the pulse method provides the time-resolved images as those shown in Fig. 4 *a–c*, which are useful to intuitively assess the data while the experiments are still in progress. We would refrain from further comparison of these two methods because the applications of both methods to fluorescence microscopy have not sufficiently matured for meaningful discussion. (The actual applications of the phase method to fluorescence microscopy we found in the literature are only those by Piston et al. (30) and Clegg et al. (31) in a meeting proceedings (unrefereed). In these reports, flimscopy was discussed and preliminary data that indicated flimscopy capability were presented, but no flimscopy image was shown.)

CONCLUSIONS

We have described a new fluorescence lifetime imaging microscopy (flimscopy). With the instrument described here, flimscopy is now possible using an accumulation time of just ≈ 30 s for ≈ 300 NBD molecules/μm^2, thereby making flimscopy feasible for biological samples. The spatial resolution is largely limited by light diffraction (≈ 250 nm) and not by the electronics of the detection system. In addition, flimscopy was shown to be a useful investigative tool for studies of intracellular processes such as endosome fusion. Further reduction in the data acquisition time may be necessary to observe faster biological processes, and the project to enhance the instrument's sensitivity is in progress in our laboratory.

The development of microscopy has depended upon the introduction of new methods of image contrast. In flimscopy, the spatial variation of fluorescence lifetime in a single cell is used to generate the image contrast. Therefore, this method initiates the development of a new generation of fluorescence microscopy.

Since time-resolved fluorescence measurements are sensitive to molecular dynamics and interactions, flimscopy allows the molecular information to be visualized in single cells. The wealth of molecular information the fluorescence lifetime decays provide, coupled with the high sensitivity and spatial resolution of the developed instrument, makes flimscopy a practical and valuable investigative tool for cell research.

Flimscopy is particularly suited to visualization of the extent of resonance energy transfer, which is one of the most important applications of spectrofluorimetry to biological problems (32–36). Using flimscopy to investigate the early stages of the endocytic pathway has revealed extensive fusion between primary endocytic vesicles and/or between sorting endosomes. Flimscopy may also be useful in detecting the association and assembly of proteins in membranes and cellular matrices. It is concluded that flimscopy is a powerful, noninvasive technique for studying a variety of processes occurring in single cells in culture and for advancing studies of in situ biophysics and biochemistry using cells and tissues.

We thank Messrs. Mitsunori Nishizawa, Naoto Oishi, Yasutoshi Ohnishi, Musubu Koishi, Masaki Kashiwasake, and Tsuyoshi Hayakawa of Hamamatsu Photonics K.K. for their technical assistance in developing the flimscopy instrument, and Drs. Tony Wilson and Michael P. Sheetz for critical reading of the manuscript.

Received for publication 31 August and in final form 28 October 1992.

REFERENCES

1. Oida, T., Y. Sako, and A. Kusumi. 1990. Fluorescence lifetime imaging microscopy (FLIM). *In* Abstracts for the 28th Annual Meeting of the Biophysical Society of Japan (in Japanese). *Biophysics.* 30:S146.
2. Oida, T., Y. Sako, and A. Kusumi. 1991. Development of fluorescence lifetime imaging microscopy (FLIM) and its application to observation of endosome fusion in single cells. *Cell Struct. Funct.* 16:609.
3. Oida, T., Y. Sako, and A. Kusumi. 1992. Fluorescence lifetime imaging microscopy (FLIM) of endosome fusion in single cells. *Mol. Biol. Cell* 3:115*a*. (Abstr.)
4. Fernandez, S. M., and R. D. Berlin. 1976. Cell surface distribution of lectin receptors determined by resonance energy transfer. *Nature (Lond.).* 264:411–415.
5. Herman, B. A., and S. M. Fernandez. 1982. Dynamics and topographical distribution of surface glycoproteins during myoblast fusion: a resonance energy transfer study. *Biochemistry.* 21:3275–3283.
6. Kusumi, A., A. Tsuji, M. Murata, Y. Sako, A. C. Yoshizawa, S. Kagiwada, T. Hayakawa, and S. Ohnishi. 1990. Development of time-resolved microfluorimetry and its application to studies of cellular membranes. *In* Time-Resolved Laser Spectroscopy in Biochemistry II. J. R. Lakowicz, editor. SPIE Press, Bellingham, WA. 776–783.
7. Kusumi, A., A. Tsuji, M. Murata, Y. Sako, A. C. Yoshizawa, S. Kagiwada, T. Hayakawa, and S. Ohnishi. 1991. Development of a streak-camera-based time-resolved microscope fluorimeter and its application to studies of membrane fusion in single cells. *Biochemistry.* 30:6517–6527.
8. Lakowicz, J. R. 1983. Principles of fluorescence spectroscopy. Plenum Press, New York.
9. Sacchi, C. A., O. Svelto, and G. Prenna. 1974. Pulsed tunable lasers in cytofluorometry. *Histochem. J.* 6:251–258.
10. Andreoni, A., A. Longoni, C. A. Sacchi, and O. Svelto. 1980. Laser fluorescent microirradiation: a new technique. *In* The Biomedical Laser: Technology and Clinical Applications. L. Goldman, editor. Springer, New York. 69–83.
11. Docchio, F., A. Longoni, R. Ramponi, C. A. Sacchi, G. Bottiroli, and I. Freitas. 1982. Recent advances in laser fluorescence microscopy. *Proc. SPIE.* 369:16–21.
12. Bottiroli, G., P. G. Cionini, F. Docchio, and C. A. Sacchi. 1984. In situ evaluation of the functional state of chromatin by means of quinacrine mustard staining and time-resolved fluorescence microscopy. *Histochem. J.* 16:223–233.
13. Herman, B. A., and S. M. Fernandez. 1978. Changes in membrane dynamics associated with myogenic cell fusion. *J. Cell. Physiol.* 94:253–264.
14. Herman, B. A., and S. M. Fernandez. 1979. A microfluorimetric study of membrane dynamics during development of dystrophic muscle in vitro. *Arch. Biochem. Biophys.* 196:430–435.
15. Alsins, J., S. Claesson, and H. Elmgren. 1982. A simple instrumentation for measuring fluorescence lifetimes of probe molecules in small systems. *Chimica Scripta.* 20:183–187.
16. Minami, T., M. Kawahigashi, Y. Sakai, K. Shimamoto, and S. Hirayama. 1986. Fluorescence lifetime measurements under a microscope by the time-correlated single-photon counting technique. *J. Luminesc.* 35:247–253.
17. Kusumi, A., A. Tsuji, M. Murata, Y. Sako, A. C. Yoshizawa, and S. Ohnishi. 1988. Development of a time-resolved microfluorimeter with a synchroscan streak camera and its application to studies of cell membranes. *In* Time-Resolved Laser Spectroscopy in Biochemistry. J. R. Lakowicz, editor. SPIE Press, Bellingham, WA. 350–351.
18. Lakowicz, J. R., and K. W. Berndt. 1991. Lifetime-sensitive fluorescence imaging using an rf phase-sensitive camera. *Rev. Sci. Instrum.* 62:1727–1734.
19. Wang, X. F., T. Uchida, D. M. Coleman, and S. Minami. 1991. A two-dimensional fluorescence lifetime imaging system using a gated image intensifier. *Applied Spectroscopy* 45:360–366.
20. Marriott, G., R. M. Clegg, D. J. Arndt-Jovin, and T. M. Jovin. 1991. Time-resolved imaging microscopy. Phosphorescence and delayed fluorescence imaging. *Biophys. J.* 60:1374–1387.
21. Johnson, P., and P. B. Garland. 1982. Fluorescent triplet probes for measuring the rotational diffusion of membrane proteins. *Biochem. J.* 203:313–321.
22. Dunn, W. A., A. L. Hubbard, N. N. Aronson, Jr. 1980. Low temperature selectively inhibits fusion between pinocytic vesicles and lysosomes during heterophagy of ^{125}I-asialofetuin by the perfused rat liver. *J. Biol. Chem.* 255:5971–5978.
23. McKinnon, A. E., A. G. Szabo, and D. R. Miller. 1977. The deconvolution of photoluminescence data. *J. Phys. Chem.* 81: 1564–1570.
24. Salzman, N. H., and Maxfield, F. R. 1988. Intracellular fusion of sequentially formed endocytic compartments. *J. Cell Biol.* 106:1083–1091.
25. Hopkins, C. R., A. Gibson, M. Shipman, and K. Miller. 1990. Movement of internalized ligand-receptor complexes along a continuous endosomal reticulum. *Nature (Lond.).* 346:335–339.
26. De Brabander, M., R. Nuydens, H. Geerts, and C. R. Hopkins. 1988. Dynamic behavior of the transferrin receptor followed in living epidermoid carcinoma (A431) cells with nanovid microscopy. *Cell Motil. Cytoskel.* 9:30–47.
27. Griffiths, G., and J. Gruenberg. 1991. The arguments for pre-existing early and late endosomes. *Trends Cell Biol.* 1:5–9.
28. Murphy, R. 1991. Maturation models for endosome and lysosome biogenesis. *Trends Cell Biol.* 1:77–82.
29. Dunn, K. W., and F. R. Maxfield. 1992. Delivery of ligands from sorting endosomes to late endosomes occurs by maturation of sorting endosomes. *J. Cell Biol.* 117:301–310.
30. Piston, D. W., D. R. Sandison, and W. W. Webb. 1992. Time-resolved fluorescence imaging and background rejection by two-photon excitation in laser scanning microscopy. *In* Time-Resolved Laser Spectroscopy in Biochemistry III. J. R. Lakowicz, editor. SPIE Press, Bellingham, WA. 379–389.
31. Clegg, R. M., B. Feddersen, E. Gratton, and T. M. Jovin. 1992. Time resolved imaging fluorescence microscopy. *In* Time-Resolved Laser Spectroscopy in Biochemistry III. J. R. Lakowicz, editor. SPIE Press, Bellingham, WA. 448–460.
32. Stryer, L. 1978. Fluorescence energy transfer as a spectroscopic ruler. *Annu. Rev. Biochem.* 47:819–846.
33. Uster, P. S., and R. E. Pagano. 1986. Resonance energy transfer microscopy: observation of membrane-bound fluorescent probes in model membranes and in living cells. *J. Cell Biol.* 103:1221–1233.
34. Watts, T. H., H. E. Gaub, and H. M. McConnell. 1986. T-cell-mediated association of peptide antigen and major histocompatibility complex protein detected by energy transfer in an evanescent field. *Nature (Lond.).* 320:179–181.
35. Herman, B. 1989. Resonance energy transfer microscopy. *Meth. Cell Biol.* 30:219–243.
36. Adams, S. R., A. T. Harootunian, Y. J. Buechler, S. S. Taylor, and R. Y. Tsien. 1991. Fluorescence ratio imaging of cyclic AMP in single cells. *Nature (Lond.).* 349:694–696.